

**CONDITIONS FOR FORMATION OF CHALCOPYRITE IN THE RUMURUTI CHONDRITES.** K. E. Miller, M. S. Thompson, D. S. Lauretta, and T. J. Zega, Lunar and Planetary Laboratory, University of Arizona, Tucson, AZ 85721, USA. kemiller@lpl.arizona.edu

**Introduction:** The Rumuruti chondrites (RCs) are a distinctive group of meteorites characterized by low metal and Fe-rich olivine, reflecting their oxidized nature [1, 2], and abundant sulfides, reflecting their high sulfidation state [3, 7]. Their bulk composition is similar to that of the ordinary chondrites [1], while their chondrule to matrix ratio more closely resembles that of the carbonaceous chondrites [4]. The RCs are classified as petrologic grades 3-6 [4], suggesting thermal alteration but not aqueous alteration. However, the R6 chondrite LaPaz Icefield (LAP) 04840 contains amphibole and biotite, suggesting high-temperature hydrous alteration that is distinct from the dry thermal metamorphism characteristic of ordinary chondrites [3].

Although extremely common as a hydrothermal product in terrestrial settings, chalcopyrite ( $\text{CuFeS}_2$ ) is very rare in meteorites. It has previously been reported in some iron meteorites [5], in the CK chondrites [6], and in the RCs [7, 8]. These limited occurrences of chalcopyrite suggest a narrow range of conditions for formation and evolution of the parent-body host, but an in-depth study of the possible origins of chalcopyrite in meteorites has not been published. We present here a study of chalcopyrite in the RCs, and an analysis of the conditions in which the observed chalcopyrite assemblages are thermodynamically stable.

**Samples:** Three RCs were chosen for study. Mount Prestrud (PRE) 95411 is an R3 chondrite, and was the first meteorite in which our group observed chalcopyrite [7]. Northwest Africa (NWA) 7514, an R5 chondrite, was chosen because it is one of the most unweathered RCs [9]. Pecora Escarpment (PCA) 91002, an R3.8-6 chondrite, was chosen because of previous reports of Cu metal grains [10].

**Methods:** Using a Cameca SX100 electron microprobe, X-ray maps of major elements and Cu were made for each sample. Points with high Cu concentrations were identified and their major element stoichiometry was determined using WDS analysis.

An electron-transparent cross section of the largest chalcopyrite grain in PRE 95411 (Assemblage A, 30  $\mu\text{m}$  in length) was removed using an FEI Helios 600i focused-ion-beam scanning-electron microscope (FIB-SEM) [11, 12]. The FIB sections were examined using two transmission electron microscopes (TEM): a 200 keV FEI Osiris ChemiSTEM and a 200 keV JEOL 2200FS.

Thermodynamic analyses were performed for three different formation scenarios. The first scenario is via a gas-solid reaction in the solar nebula and was tested using the HSC Chemistry 5.1 software package to calculate the equilibrium temperature for the reaction  $\text{Cu}(s) + \text{Fe}(s) + 2\text{H}_2\text{S}(g) = \text{CuFeS}_2(s) + 2\text{H}_2(g)$  at solar  $\text{H}_2\text{S}/\text{H}_2$  ratios. Since Cu occurs as a pure phase in the ordinary chondrites [13], the Cu reactant was assumed to be metallic Cu.

The second scenario assessed was the relative thermodynamic stability of Cu metal and chalcopyrite in an aqueous fluid in equilibrium with  $\text{Fe}_{0.877}\text{S}$ . The HSC Chemistry 5.1 equilibrium composition module was used to determine the stable species at 250 temperature steps between 250 and 1000 K. Pressure was varied from 1 to 1000 bars, and the Cu/Fe and Cu/S ratios were varied from 0.01 to 1 to determine the circumstances in which Cu was present in chalcopyrite but not as Cu metal.

The final scenario that was examined was crystallization from a melt, followed by equilibration. The bulk composition of the Cu, Fe, and S in Assemblage A was calculated assuming that the composition measured in the exposed surface was representative of the assemblage as a whole. This bulk composition was compared to Cu-Fe-S ternary phase diagrams [14]. The temperature at which the predicted mineral phases matched the observed mineral phases was determined.

**Results:** In PRE 95411, 12 grains of chalcopyrite were found. Nine chalcopyrite grains were found in NWA 7514, whereas three grains of chalcopyrite and one grain with a composition close to cubanite ( $\text{CuFe}_2\text{S}_3$ ) were found in PCA 91002. Metallic Cu was not identified in any of the analyses.

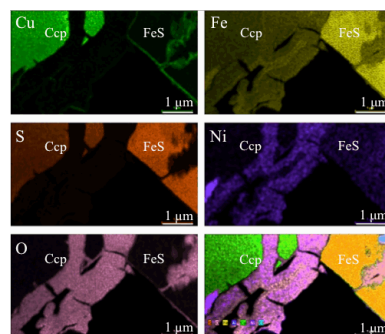


**Fig. 1.** X-ray maps from FIB-TEM of Assemblage A; chalcopyrite (Ccp) and iron sulfide (FeS) grains as labeled; bottom right shows a composite of individual element maps.

FIB-TEM analysis of Assemblage A confirms the crystal structure of chalcopyrite and an adjacent iron sulfide grain. X-ray maps of the FIB section reveal the presence of an O-, Ni-, and Fe-rich vein between the

chalcopyrite and iron sulfide, and the presence of a Cu rim lining the iron sulfide grain (Fig. 1).

The equilibrium temperature for chalcopyrite formation via gas-solid reaction is 598 K using solar values for the H and CI chondrite values for the S abundance [15]. These values give  $H_2S/H_2 = 30.9 \times 10^{-6}$ .

In an aqueous setting, Cu is stable in chalcopyrite but not metallic Cu at 1 bar with a Cu/S ratio of 0.1 and Cu/Fe ratios from 0.01-0.1 below 446 K, and pH above 5.33 (Fig. 2). At pressures between 10 and 1000 bars and Cu/S and Cu/Fe ratios of 1, chalcopyrite was stable below 459 K, consistent with experimental studies of Cu-sulfide synthesis in chondrites [16].

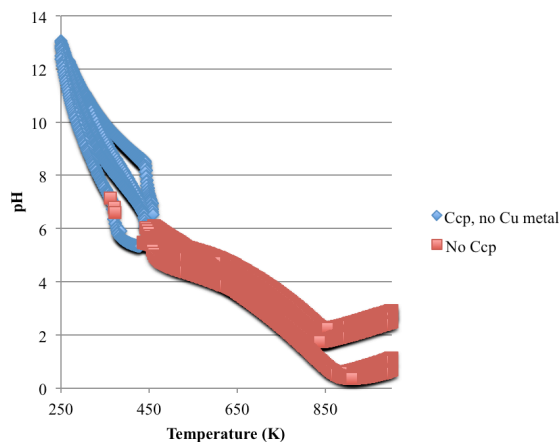


**Fig. 2.** Aqueous conditions tested for chalcopyrite (Ccp) stability; conditions: 1 bar, Cu/S = 0.1, Cu/Fe = 0.01-0.1; 10-1000 bar, Cu/S = Cu/Fe = 1.

The bulk abundances in Assemblage A are 4% Cu, 57% Fe, and 39% S. At 473 K, the assemblage predicted by ternary diagrams matches observations (Fig. 3). Equilibration at this temperature is expected to produce 87% pyrrhotite and 13% chalcopyrite. The observed assemblage is 89% pyrrhotite and 11% chalcopyrite.

**Discussion:** Using the weathering index for RCs [17], the sections examined are wi-0, or unweathered, (NWA 7514 and PCA 91002) and wi-2, or moderately weathered (PRE 95411). However, even in PRE 95411 chalcopyrite is found equally in the areas where brown-staining of the silicates suggests terrestrial weathering and in areas free of staining and essentially unweathered. From this, we conclude that chalcopyrite is the product of extraterrestrial processes.

The vein structure found between chalcopyrite and iron sulfide in the FIB transect (Fig. 1) resembles a similar structure present in cubanite from the Orgueil CII meteorite, in which it was attributed to aqueous processes [11]. The uniformity of the Cu rim surrounding the iron sulfide and outlining the oxide incursion into the grain suggests deposition by a fluid.

The assemblage predicted to crystallize from a melt and continue to equilibrate down to 473 K closely matches Assemblage A in both the mineral phases observed and their relative abundances. In this scenario, at 773 K, the assemblage would consist of cubanite, pyrite, and pyrrhotite. At 607 K, chalcopyrite becomes stable in the presence of pyrrhotite, and at 583 K monoclinic pyrrhotite becomes stable. Below 412 K, troilite and pyrrhotite stably coexist [14]. With one exception, the chalcopyrite-sulfide assemblages observed in the RCs are isolated in matrix and not associated with chondrules, which are the most evident melt products present.

We conclude that chalcopyrite in the RCs is either an aqueous or melt crystallization product.

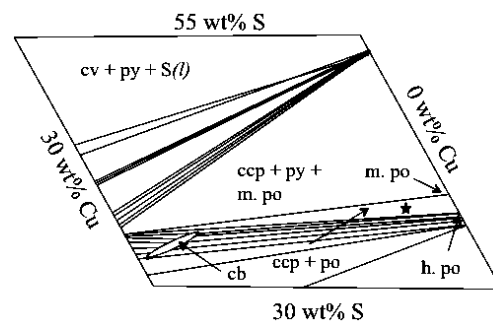


**Fig. 3.** Cu-Fe-S ternary at 473 K [14]; the composition of Assemblage A is the star; minerals are covellite (cv), pyrite (py), chalcopyrite (ccp), monoclinic (m.) and hexagonal (h.) pyrrhotite (po), and cubanite (cb).

**References:** [1] Kallemeyn G. W. et al. (1996) *Geochim. Cosmochim. Ac.*, 60, 2243-2256. [2] Righter K. and Neff K. E. (2007) *Polar Science*, 1, 25-44. [3] McCanta M. C. et al. (2008) *Geochim. Cosmochim. Ac.*, 72, 5757-5780. [4] Bischoff A. et al. (2011) *Chemie der Erde*, 71, 101-133. [5] Buchwald V. F. (1977) *Phil. Trans. R. Soc. Lond. A.*, 286, 453-491. [6] Geiger T. and Bischoff A. (1995) *Planet. Space Sci.*, 43, 485-498. [7] Jackson K. M. and Laretta D. S. (2010) *73<sup>rd</sup> Annual Meteoritical Society Meeting*, Abstract #5164. [8] Schulze H. et al. (1994) *Meteoritics*, 29, 275-286. [9] Ruzicka A. et al. (2013) *LPS XXXIV*, Abstract #1168. [10] Rubin A. E. and Kallemeyn G. W. (1994) *Meteoritics*, 29, 255-264. [11] Berger E. L. et al. (2011) *Geochim. Cosmochim. Ac.*, 75, 3501-3513. [12] Zega T. J. et al. (2007) *Meteoritics & Planet. Sci.*, 42, 1373-1386. [13] Rubin A. E. (1994) *Meteoritics*, 29, 93-98. [14] Kullerud G. et al. (1969) *Econ. Geol. Monogr.*, 4, 323-343. [15] Lodders K. (2003) *Ap. J.*, 591, 1220-1247. [16] Berger, E. L. (2011) Ph.D. Thesis, The University of Arizona. [17] Rubin A. E. and Huber H. (2005) *Meteoritics & Planet. Sci.*, 40, 1123-1130.